Aggregation Patterns in Stressed Bacteria

Lev Tsimring and Herbert Levine
Institute for Nonlinear Science, University of California at San Diego, La Jolla, California 92093-0402

Igor Aranson
Deptartment of Physics, Bar-Ilan University, Ramat Gan, Israel

Eshel Ben-Jacob, Inon Cohen, and Ofer Shochet
School of Physics and Astronomy, Raymond & Beverly Sackler Faculty of Exact Sciences, Tel-Aviv University, Tel-Aviv 69978, Israel

William N. Reynolds
Complex Systems Division, Los Alamos National Laboratory, Los Alamos, New Mexico
(Received 24 February 1995)

We study the formation of spot patterns seen in bacterial colonies when the bacteria are subjected to oxidative stress due to hazardous by-products of respiration. The cell density is coupled to a chemoattractant concentration as well as to nutrient and waste fields. The model combines the propagation of a front of motile bacterial radially outward from an initial site, a Turing instability of the uniformly dense state, and a reduction of motility for cells sufficiently far behind the front. The wide variety of patterns seen in the experiments is reproduced by the model by varying the details of the initiation of the chemoattractant emission as well as the transition to a nonmotile phase.

PACS numbers: 87.10.+e, 47.20.Hw

Over the past few years, there has been a significant increase in our understanding of how spatial patterns emerge via the propagating interfacial dynamics of nonequilibrium systems [1,2]. We have discovered how seemingly different systems can nonetheless exhibit strikingly similar behavior, due to the existence of nonequilibrium pattern selection principles. These principles rely on the idea that the final structure which emerges from an initially (linearly) unstable state is affected mostly by the nature of the instability, the possible existence of stable, highly nonequilibrium isolated steady-state structures (such as the single dendrite in nonequilibrium solidification), and the competition between globally ordered arrangements of these structures as compared to more disordered morphologies. This framework has been applied to a variety of systems of physical, chemical, and, most recently [3], biological interest.

In this work [4], we analyze spot and stripe patterns seen in bacterial growth experiments; the first such results were due to Berg and Budrene [5] in *e. coli*. They found that cells could aggregate chemotactically, resulting in a wide variety of different colony structures ranging from arrays of spots to radially oriented stripes to arrangements of more complex elongated spots. In their study, *e. coli* were grown on single carbon source media, and the appearance of patterns only in the case of a highly oxidized nutrient suggested that respiratory by-products (leading to oxidative stress [6]) trigger the observed chemotactic behavior. Two of their figures are reproduced in Fig. 1. It is worth noting that this class of patterns is not limited to *e. coli*; similar structures have been seen in *Salmonella typhimurium* [7] and in *Bacillus subtilis* [8]. We suspect that this class of patterns is a universal "possibility" for microbial systems aggregating in the face of adversity.

Normally, bacteria divide and spread out into regions of initially low density. This can take the form of an expanding circle [9], or if some metabolic factor is in short supply, a (set of) expanding ring(s) [10]. In the presence of the aforementioned oxidative stress, the bacteria begin to emit a chemoattractant (believed to be aspartate) which causes them to aggregate via biasing their motion. Eventually, the bacteria turn nonmotile, freezing the pattern into place. From the modeling point of view, the coupling of the chemoattractant diffusion equation to the bacterial density evolution leads to a Turing-like instability of the uniform density state. If we were to start the entire system at uniform bacterial density, patterns would develop as soon as the concentration of waste reaches a threshold value. These patterns would be defect ridden, governed by the precise details of the initial conditions. This is indeed what was observed in the case of the purposeful addition of hydrogen peroxide. The symmetric structures seen during growth from a single inoculated site are thus due to the interplay of the expansion with the Turing instability as triggered by the waste field, and possibly autocatalytically by the attractant field itself. Below, we will see how this occurs within our model.

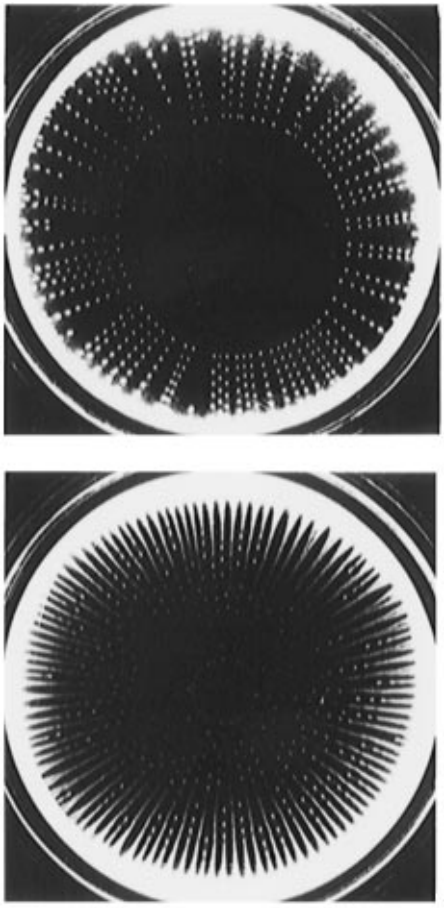

FIG. 1. Two examples of patterns of bacteria *e. coli* in experiments by Budrene and Berg [1]: radial alignment of spots (a), radially oriented stripes (b).

Based on the above, we propose the following set of continuum equations for this system [11]:

$$\dot{\rho} = D_\rho \vec{\nabla}^2 \rho + G(\rho, n) - v_c \vec{\nabla} \cdot (\rho \vec{\nabla} c) - I[w]\rho\,, \quad (1)$$

$$\dot{\rho_n} = I[w]\rho \quad (2)$$

$$\dot{n} = D_n \vec{\nabla}^2 n - \alpha \rho n\,, \quad (3)$$

$$\dot{w} = D_w \vec{\nabla}^2 w + \alpha_w \rho n - (\beta_w + \gamma\rho) w\,, \quad (4)$$

$$\dot{c} = D_c \vec{\nabla}^2 c + T[w, c]\rho - \beta_c c\,. \quad (5)$$

Here ρ and ρ_n are densities of motile and nonmotile bacteria, w is a concentration of respiratory waste products, c is the chemoattractant concentration which is emitted by the bacterium, and n is the nutrient which is eaten by bacteria.

Equation (1) contains a growth term which we typically take to be of the form $G = r\rho^p n/(n + n_0) - g\rho^3$, with $p \simeq 1$ [12]; this form reflects the nutrient-inhibited growth of cells at a low food concentration and a finite reproduction rate which is achieved in a "nutrient-rich" limit. At high density of bacteria the growth is limited by the nonlinear term $-g\rho^3$. Motion is governed by diffusion and by a chemotactic term representing the response of the bacteria to a gradient in the attractant. The strength of the chemotactic response is determined by the coefficient v_c. As already mentioned, it is important to incorporate the fact that sufficiently far behind the advancing front, the bacteria differentiate into a nonmotile form (term $I[w]\rho$ in Eqs. (1) and (2). We assume that the transition occurs due to the accumulation of effects due to starvation; specifically, the transition to the nonmotile phase occurs when $n_c \equiv \int_0^t (n_0 - n)\theta(n_0 - n)\, dt$ exceeds some threshold value n_{tr}, i.e., by setting $I[w] = \delta\Theta(n_c - n_{tr})$ [13] [$\Theta(x)$ is the Heaviside function]. Depletion of food is described by Eq. (3), it is assumed that the rate of consumption is proportional to the density of bacteria *and* the concentration of food itself, so it never becomes negative. The rate of waste accumulation is proportional to the nutrient consumption term [Eq. (4)], and we assume that the waste decomposes with a rate dependent on the bacterial density, as this is, in fact, the underlying reason for the bacteria to aggregate. Finally, the emission of chemoattractant c is proportional to the local density of bacteria, and it is triggered by local waste field; specifically, we assume that the chemoattractant is emitted if either $w > w_0$ and $c > c_0$ or $w > w_1$, where $w_1 > w_0$ (formally, $T[w, c] = g_c \mathrm{sgn}\,[\Theta(w - w_0)\Theta(c - c_0) + \Theta(w - w_1)]$). The difference between w_1 and w_0 represents the possible autocatalytic behavior of the attractant. The last term in Eq. (5) describes experimentally documented decomposition of chemoattractant.

To understand the structure of our model, it is convenient to first consider the case of a constant uniform nutrient ($n \gg n_0, \alpha = 0$) and in the absence of any waste effects (i.e., $T = 1$). The system now has an unstable steady state $\rho = c = 0$. If we start with an initial condition of localized bacteria density amidst a sea of $\rho = 0$, the density will spread. In the absence of coupling to c, the equation for density takes a form of the Kolmogorov-Petrovsky-Piskunov equation for which it is well known that the front would move at a speed $2\sqrt{D_\rho r}$ via the usual marginal stability criterion [14]. By continuity, the front will continue to expand as long as v_c is not too large. On the other hand, the nontrivial uniform state is given by $\rho = \sqrt{r}, c = 1/\beta$. The stability of this state to perturbations with wave vector q is given by the roots of

$$(\omega + D_\rho q^2 + 2r)(\omega + D_c q^2 + \beta_c) = v_c r^{1/2} q^2. \quad (6)$$

It is easy to see that for large enough chemotactic response v_c this system has a band of wave vectors with purely real and positive growth rates ω. The instability is generated by the chemotactic term in (1), which in the linear approximation provides negative cross-diffusivity. In this respect it differs from the usual Turing instability, as the latter require different diagonal diffusivities D_ρ vs D_c. Combining these arguments leads one to expect that generically there exists an intermediate range of v_c for which the bacteria density will propagate outward and create an expanding Turing-unstable region. Adding the nutrient field back in does not alter the above conclusions in any qualitatively important manner. The importance of waste dynamics will be discussed below.

To simulate the above equations, we used a split-step spectral code on a 128×128 lattice; specifically, the linear parts of the evolution were treated by fast Fourier transforms and the nonlinear pieces by explicit finite differences. Lattice anisotropy which comes primarily from discretizing the chemotactic term in Eq. (1) was minimized by computing it simultaneously on two lattices which differ by 45° rotation [15]. We can immediately verify the above simple features and proceed to discuss the formation of complex ordered structures.

Let us first focus on colony dynamics in the absence of a threshold for chemoattractant emission [$T(w, c) \equiv 1$]. In Figure 2, we show a snapshot of a typical simulation of the model equations. As the interface propagates outwards, it creates a set of concentric rings. The breakup of the rings into spots occurs somewhere behind the front, dependent on the specific value of υ_c; for small enough υ_c, the rings do not break up. Ordered arrangements of the spots are hard to achieve, since the interaction between different rings is extremely small. Moreover, the appearance of a number of rings behind the outer rings is not in accord with the Budrene and Berg experiment. In most cases the spots appeared right behind the outer ring.

To account for this effect, we impose the threshold for chemoattractant emission. The existence of this strong nonlinearity makes the rear part of the outer ring extremely sensitive to the structure of the waste and chemical fields. In particular, the emission is triggered preferentially at certain angular positions as opposed to along an entire ring. This then can cure the two previous problems—proper thresholding can lead directly to spots and previous spots strongly bias the formation of new spots. In Fig. 3, we show the results of full model simulations, showing significantly improved agreement with experiment. We now discuss in turn the threshold choices that lead to the differing results in Fig. 3.

In Fig. 3(a), we see that spots form at positions such that they will eventually form radial rows; these rows are quite similar to those in the experimental pattern in

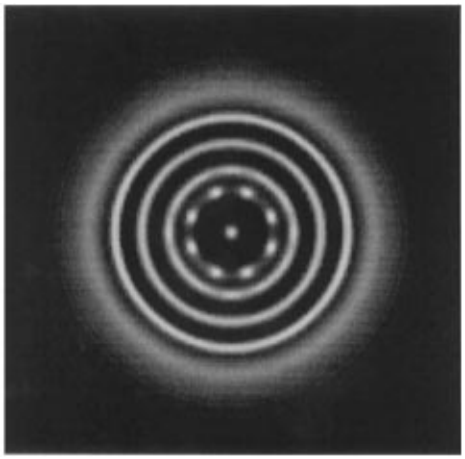

FIG. 2. A snapshot of bacteria density ($\rho + 0.5\rho_n$) at $t = 18$ within the model with $D_n = 0.4, D_c = 0.2, D_w = 0.4$, $\alpha = 0.12$, $r = 1.8$, $\beta_c = g = g_c = 1$, $\alpha_w = 0.3$, $\beta_w = 0.1$, $\gamma = 0.2$, $n_0 = 0.5, n_{tr} = 0.03$, $\delta = 0.5$, and $\upsilon_c = 6.0$, thresholds for chemoattractant disabled, system size is 40, time step 0.02. Concentric rings are formed in the wake of the outer ring.

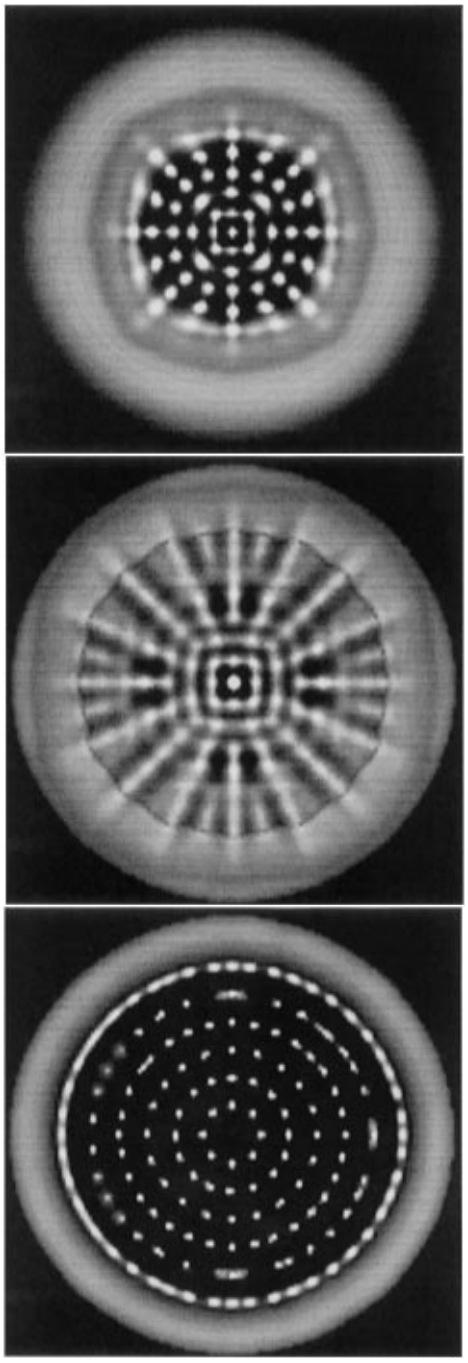

FIG. 3. (a) Same as in Fig. 2 but with enabled thresholds ($w_0 = 0.3, w_1 = 0.55, c_0 = 0.04$) and $\upsilon_c = 7$; radial rows of spots are clearly seen [cf. Fig. 1(a)]. *(b)* Same as in (a) but with weaker chemotaxis ($\upsilon_c = 6$), radial stripes similar to Fig. 1(b) are seen. (c) Pattern of $\rho + 0.5\rho_n$ within the model (1)–(5) with different thresholds ($w_0 = 0.3, w_1 = 0.5, c_0 = 0.5$) and higher chemotaxis ($\upsilon_c = 9$), other parameters are the same as in *b*. A staggered alignment is seen far from the center.

Fig. 1(a). The reason for this is that the concentration of c in the ring of currently aggregating spots is nonuniform, and due to diffusion this inhomogeneity spreads into the rear part of the outer ring. This biases the location for the new spots so they are created right in front of the previous spots. Once the spots form, they are not allowed to move very far, since as the nutrient depletes, bacteria transform into a nonmotile phase. If the chemotactic response (v_c) is reduced, instead of radially aligned spots, radial stripes are formed; this too has been seen experimentally [see Figs. 1(b) and 3(b)]. We note in passing that the brightness of spots in experimental images is greater for motile bacteria, so in all numerical figures we show the gray scale plots of $(\rho + 0.5\rho_n)$.

In the other main experimental spot pattern, the spots arrange themselves in a manner such that the new spot appears roughly between two preexisting ones at the previous ring. By adjusting the values of c_0 and w_1 we can produce a similar pattern as well [see Fig. 3(c)]. By significantly increasing the threshold c_0 we effectively made the residual level of chemoattractant irrelevant, and instead the waste threshold w_1 plays the major role. We should note, however, that this structure seems to be missing the visually striking spirals which create the sunflower impression in the original Budrene and Berg figure [Fig. 1(a) of their paper]. Whether this difference represents a shortcoming of our model which tends to keep spots along circular rings, or, as we feel more likely, that a larger system with less anisotropy and perhaps a different set of parameters could reproduce this visual impression is a question for future work.

To summarize, we have shown how the interplay of front propagation and a Turing-type instability can lead to spot patterns similar to those observed in bacterial aggregation. We have concentrated on generic mechanisms which should remain important regardless of the details of the explicit biological interactions as these details become clearer. One important conclusion is that the biological mechanism for the "turning on" of chemotattractant emission is of critical importance in giving rise to the observed colonies. Of course, attempts at more quantitative comparison would require as input the functional dependencies of all the various pieces entering into the dynamics. We feel that this level of detailed modeling is a reasonable undertaking only after a demonstration that physics does indeed have a hope of describing what is going on without the need to invoke an incredibly complex hierarchy of biological mechanisms. This paper has been an attempt to demonstrate exactly this point and to thereby provide motivation for a future quantitative study.

[1] D. Kessler, J. Koplik, and H. Levine, Adv. Phys. **37**, 255 (1988).
[2] E. Ben-Jacob and P. Garik, Nature (London) **343**, 523 (1990).
[3] E. Ben-Jacob *et al.*, Nature (London) **368**, 46 (1994); D. Kessler and H. Levine, Phys. Rev. E **48**, 4801 (1993).
[4] Some of our ideas have appeared in Nature (London) (to be published).
[5] E. Budrene and H. Berg, Nature (London) **349**, 630 (1991).
[6] G. Storz, L. A. Tartaglia, S. B. Farr, and B. N. Ames, Trends Genet. **6**, 363 (1990).
[7] Y. Blat and M. Eisenbach, J. Bacteriology (to be published).
[8] E. Ben-Jacob and O. Shochet (unpublished).
[9] J. Shapiro, Physica (Amsterdam) **49D**, 214 (1991).
[10] J. Adler, Science **153**, 708 (1966); R. Nossal, Exp. Cell Res. **75**, 138 (1972); A. Wolfe and H. Berg, Proc. Nat. Acad. Sci. U.S.A. **86**, 6973 (1989).
[11] The only previous work to date on this system used a simple model without thresholds; W. J. Bruno, Los Alamos CNLS Newsletter **82**, 1 (1992); (private communication).
[12] The idea of using $p > 1$ to account for the discrete character of an aggregating particle (here a bacterium) arose in the context of diffusion-limited aggregation; see E. Brener, H. Levine, and Y. Tu, Phys. Rev. Lett. **66**, 1978 (1991).
[13] Strictly speaking, the integrated nutrient deficit should be done in "Lagrangian" variables, i.e., finding the nutrient deficit for individual bacteria as they move through space. This is hard to implement in our "Eulerian" description and in any case should be a small effect, since in our model bacteria do not move over distances over which there are significant changes in nutrient concentration.
[14] W. Van Saarloos, Phys. Rev. A **39**, 6327 (1989), and references therein. This actually applies only to the case $p = 1$, but as long as p is not too large, the selected velocity changes only slightly from the marginal stability prediction.
[15] The effect of residual anisotropy was determined by letting the system evolve for some time, rotating the fields by an irrational angle, and then continuing the time evolution. This procedure did not interfere with the radial row structure discussed later in the text.